Environ. Sci. Technol. **2007**, *41,* 1016−1023

Optimization of Metalworking Fluid Microemulsion Surfactant Concentrations for Microfiltration Recycling

FU ZHAO,[†] ANDRES CLARENS,[‡] AND STEVEN J. SKERLOS*,[†]

Environmental and Sustainable Technologies Laboratory, Departments of Mechanical Engineering and Civil and Environmental Engineering, University of Michigan at Ann Arbor, Ann Arbor, Michigan 48109-2125

Microfiltration can be used as a recycling technology to increase metalworking fluid (MWF) life span, decrease procurement and disposal costs, and reduce occupational health risks and environmental impacts. The cost-effectiveness of the process can be increased by minimizing fouling interactions between MWFs and membranes. This paper reports on the development of a microfiltration model that establishes governing relationships between MWF surfactant system characteristics and microfiltration recycling performance. The model, which is based on surfactant adsorption/desorption kinetics, queueing theory, and coalescence kinetics of emulsion droplets, is verified experimentally. An analysis of the model and supporting experimental evidence indicates that the selection of surfactant systems minimally adsorb to membranes and lead to a high activation energy of coalescence results in a higher MWF flux through microfiltration membranes. The model also yields mathematical equations that express the optimal concentrations of anionic and nonionic surfactants with which microfiltration flux is maximized for a given combination of oil type, oil concentration, and surfactant types. Optimal MWF formulations are demonstrated for a petroleum oil MWF using a disulfonate/ethoxylated alcohol surfactant package and for several vegetable oil MWFs using a disulfonate/ethoxylated glyceryl ester surfactant package. The optimization leads to flux increases ranging from 300 to 800% without impact on manufacturing performance. It is further shown that MWF reformulation efforts directed toward increasing microfiltration flux can have the beneficial effect of increasing MWF robustness to deterioration and flux decline in the presence of elevated concentrations of hardwater ions.

1. Introduction

Metalworking fluids (MWFs) serve to reduce friction and temperature in metal cutting and forming operations (*1*, *2*). The use of MWFs generally extends the life of tools, increases production rates, and improves the surface finish of metal products (*2*, *3*). All of these benefits have made MWFs essential to modern metals manufacturing. In recent years, MWF use has been growing around the world, with sales in North America exceeding 2 billion gallons in 2000 (*4*). As MWF use has increased, so too has an awareness of the large economic costs (*5*), occupational health risks (*6*, *7*), and environmental impacts associated with MWF systems (*8*, *9*).

Research efforts to address the economic, environmental, and health issues of MWF systems have generally centered around (1) reducing or eliminating MWF use in manufacturing (*10*), (2) formulating MWFs to better withstand in-process deterioration (*3*, *11*), and (3) improving waste treatment methods (*12*−*14*). In addition to these efforts, several research groups are also investigating advanced MWF recycling approaches based upon membrane filtration (*15*−*18*). Membrane filtration recycling of MWFs can lower manufacturing costs and environmental impact by reducing disposal and acquisition frequencies while simultaneously removing the microbial contamination that can lead to occupational health risks and MWF deterioration (*16*, *17*).

Previous research has demonstrated that microfiltration and ultrafiltration can remove microorganisms, metallic particulates, and loosely emulsified oils from MWFs (*17*, *18*). Furthermore, operating strategies for minimizing membrane fouling due to the build-up of these contaminants have been well-established using techniques such as cross-flow filtration (*19*), backpulsing (*20*), and ultrasonic vibration (*21*). When these techniques are applied, the maximum transport rate of MWFs through membranes is typically limited by the fouling interactions that exist between MWF chemistries and membranes. Even for synthetic MWFs, which are oil-free nanodispersions or solutions, microfiltration flux rates in the absence of contaminants can be too low for profitable recycling (*16*). Previous research has shown that the careful selection of lubricant additives and defoamers in synthetic MWFs is critical to achieve profitable recycling via membrane filtration (*22*).

More recent investigations have demonstrated the possibility of utilizing membrane filtration to recycle semisynthetic MWFs (*15*, *17*, *23*). Semisynthetics comprise about 40% of the MWF market and are typically oil-in-water microemulsions with droplet sizes less than 50 nm (*3*). Generally microfiltration is used instead of ultrafiltration since semisynthetic MWF microemulsion droplets can become larger than the pore size of ultrafiltration membranes, leading to phase separation and failure of the permeated fluid as a MWF. Although microfiltration membranes allow microemulsion droplets to permeate, significant fouling and low flux have been observed in the process, even in the absence of contaminants (*23*). Recycling low-flux MWFs is generally

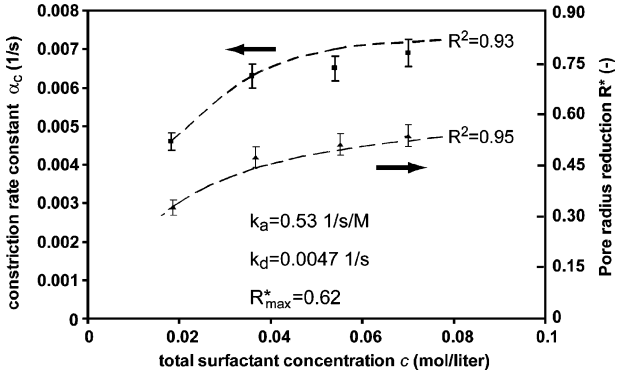

FIGURE 1. Comparison of constriction parameters (α_c and R^*) obtained from model predictions (dashed lines) and flux data (dots) for mixed surfactant solutions of SPS and DiIPA.

* Corresponding author phone: (734)615-5253; fax: (734)647-3170; e-mail: skerlos@umich.edu.
[†] Department of Mechanical Engineering.
[‡] Department of Civil and Environmental Engineering.

10.1021/es0608038 CCC: $37.00
Published on Web 12/16/2006

infeasible since it requires prohibitively large and costly microfiltration systems (*24*), and the low flux is generally indicative of difficulty to remove fouling material by economical cleaning methods.

Previous research has identified three fundamental mechanisms of flux decline during microfiltration recycling of semisynthetic MWF microemulsions: pore constriction, pore blocking, and surface film formation (*23*). It has been shown that these fouling mechanisms can be well-described by the following mathematical expression

$$J(t) = \frac{\Delta P e^{-\alpha_b t}}{R_m}[e^{-\alpha_c t} + (1 - R^*)^4(1 - e^{-\alpha_c t})] + \frac{\Delta P}{R_m}(1 - R^*)^4\left(1 - \frac{\sqrt{2}}{2}\right)\cdot(1 - e^{-\alpha_b t})\cdot \left(1 + \frac{2\Delta P \psi c_0 t}{R_m^{\,2}}(1 - R^*)^8\left(1 - \frac{\sqrt{2}}{2}\right)^2\right)^{-0.5} \quad (1)$$

where $J(t)$ is the flux of MWF through the membrane as a function of time (LMH, liters per meter squared membrane area per hour), ΔP is the pressure drop across the membrane (Pa), R_m is the membrane resistance to the flow of pure water (Pa/m/s), and c_0 is the mass concentration of fouling constituents such as oil and surfactants (kg/L). The model parameters are α_b and α_c, which are the rate constants for pore blocking and pore constriction, respectively (1/s), R^* which is the steady-state equivalent pore radius reduction (dimensionless), and ψ which is the specific surface film resistance (Pa·m·s/kg). In ref *23* it was shown that the microfiltration model expressed by eq 1 agrees closely with experimental observations ($R^2 = 0.99$), and direct evidence was provided to support the conclusion that the model parameters estimated using flux data and eq 1 are consistent with their expected physical interpretations. A brief summary of these results is provided in the Supporting Information.

While eq 1 is useful to describe the mechanisms of flux decline, it does not provide guidance regarding how MWF microemulsions can be formulated to maximize flux. We began this research with a hypothesis that if eq 1 could be modified to include sources of flux-decline such as surfactant adsorption and microemulsion droplet coalescence, it would be possible to use the modified equation to select better surfactants and optimize surfactant concentrations in MWF formulations to maximize microfiltration flux. Toward this end, this paper develops eq 1 further to include (1) the modeling of pore constriction using surfactant adsorption/desorption concepts and (2) the modeling of pore blocking using queueing theory and emulsion coalescence kinetics concepts. Experimental evidence supporting the extended model is provided along with a demonstration of how the model can be used to optimize surfactant concentrations for maximum flux during the microfiltration recycling of semisynthetic MWFs.

2. Pore Constriction Model

It has been pointed out in ref *23* that membranes are susceptible to adsorption of surfactants found in all semisynthetic MWFs, and that pore constriction occurs when the surfactant adsorption rates exceed desorption rates. For single-surfactant solutions at concentrations below their critical micelle concentration (CMC), adsorption typically occurs as a monolayer. The Supporting Information accompanying this paper demonstrates that the pore constriction rate (α_c) in eq 1 can be expressed for such monolayer adsorption as

$$\alpha_c = k_a c + k_d \quad (2)$$

where k_a is the adsorption rate (1/s/M), c is the surfactant concentration (M), and k_d is the desorption rate (1/s).

Although eq 2 adequately describes α_c as a function of a single surfactant concentration, it is not suitable for MWFs since MWF microemulsions commonly employ surfactant mixtures. Moreover, the surfactant concentrations in MWFs are generally well above their individual CMC values, leading to relatively thick adsorption layers (about 100 nm) on the pore interiors of microfiltration membranes. These adsorption layers reduce the pore area available for permeation and create drag forces that further reduce flux. As shown in ref *23*, an equivalent hydraulic pore radius reduction (R^*) can be defined that accounts for both effects on MWF flux.

To express α_c for surfactant mixtures with concentrations above their individual CMC values, we begin by assuming that the adsorption rate is proportional to the bulk surfactant concentration and that the desorption rate is proportional to the equivalent amount of surfactant already adsorbed on the membrane surface. Denoting R^*_{max} as the maximum equivalent pore radius reduction when steady-state is achieved between adsorption and desorption, equations describing the equivalent pore radius reduction R^* and the pore constriction rate constant α_c can be derived by analogy to the single surfactant case as (see the Supporting Information for details on derivation and assumptions)

$$R^* = \frac{R^*_{max} c}{k_d/k_a + c} \quad (3)$$

$$\alpha_c = 4R^*_{max}k_a c - 12\frac{(R^*_{max}k_a c)^2}{k_a c + k_d} \quad (4)$$

To verify the relationships derived in eqs 3 and 4, a mixture of MWF surfactants was microfiltered through 0.8 μm polyvinylpyrolidone coated polycarbonate membranes at molar concentrations of 0.018 M, 0.036 M, 0.054 M, and 0.072 M. The point of zero charge for the membrane material is about pH = 4.9. At the higher pH of typical MWFs (i.e., 9−10), the membrane is negatively charged which minimizes adsorption by nonionic and anionic surfactants. The surfactant mixture consisted of sodium petroleum sulfonate (SPS) as the anionic surfactant and diisopropanolamine (DiIPA) as the nonionic surfactant (*23*). These surfactants are commonly used together in MWF systems. Two experiments (0.018 M and 0.072 M) were utilized to estimate the model parameters. Using eq 1, the pore radius reductions R^* at these two concentrations were first determined. Then using eq 3, R^*_{max} and k_a/k_d were calculated to be 0.62 and 110 1/M, respectively. Using the pore constriction rate constant α_c at 0.018 M, k_a and k_d were estimated separately from eq 4 as 0.53 1/s/M and 0.0047 1/s, respectively. Using these estimated parameters, the model predicts R^* (eq 3) and α_c (eq 4) as a function of concentration with good agreement ($R^2 > 0.90$) to values estimated from experimental flux data as shown in Figure 1. The deviation falls within the experimental error of flux measurements, which is about 10%. The agreement suggests that adsorption behavior in this case is different from the case of a single surfactant with concentration below its CMC, where the adsorption rate is linearly proportional to the monomer concentration. The agreement also suggests that the approach proposed here provides a useful functional relationship to include in eq 1 to describe the pore constriction rate constant (α_c) and the maximum pore radius reduction (R^*) as a function of total surfactant concentration.

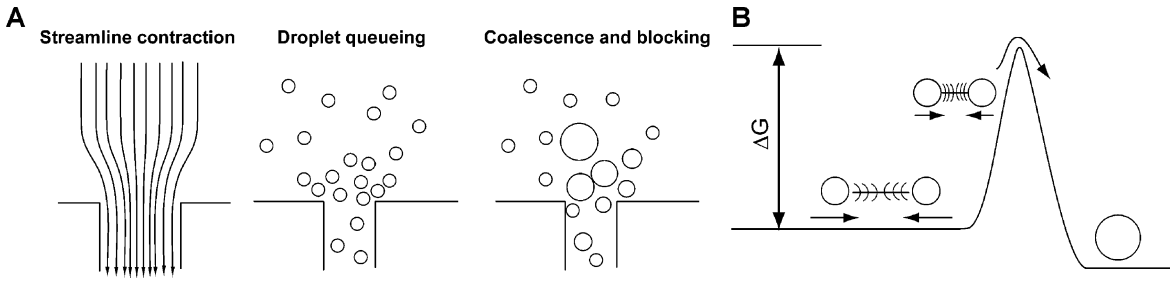

FIGURE 2. (A) Pore blocking modeled via queueing theory and coalescence kinetics. (B) Activation energy required for droplet coalescence.

3. Pore Blocking Model

The transport of microemulsion droplets through microfiltration membranes is delayed at the surface due to streamline contraction and pore constriction. This results in a "pile-up" of microemulsion droplets near the pore entrances which increases the probability of droplet collisions and coalescence. Over time, coalesced emulsion droplets are generated at the membrane surface, and these will grow in size until they are able to block pore openings (*23*).

To arrive at a model of the pore blocking rate constant (α_b) as a function of MWF formulation parameters, we have modeled the process in analogy to a queueing process with the fundamental blocking mechanism governed by coalescence kinetics as shown in Figure 2. Based on the characteristics of the microfiltration process, it can be assumed that (1) interference between pores can be neglected and (2) droplet arrivals follow a Poisson process. With these assumptions the pore blocking process can be described as an M/D/1 queuing process (*25*) where the parameters of the process are given as follows

$$\text{arrival rate } (\lambda):\ \lambda \propto c_n \cdot J \tag{5}$$

$$\text{service rate } (\mu):\ \mu \propto J(1-\beta \cdot c_n) \cdot c_n / d_p^{\,2} \tag{6}$$

$$\text{utilization factor } (\rho):\ \rho = \frac{\lambda}{\mu} \tag{7}$$

where c_n is the number of microemulsion droplets per volume (1/L), J is the flux (LMH), β is the delay factor on the service rate due to streamline contraction and pore constriction (L/droplet), and d_p is the mean droplet diameter (m).

Since the arrival of emulsion droplets at the membrane surface is very fast (about 1000 droplets per pore per second), the queue will reach its equilibrium state within a very short time period. At the equilibrium state, the probability of n droplets waiting in the queue for this M/D/1 process can be calculated as in ref *25*:

$$\begin{cases} p_0 = 1-\rho \\ p_1 = (1-\rho)(\mathrm{e}^{\rho}-1) \\ \quad \vdots \\ p_n = (1-\rho)\displaystyle\sum_{k=1}^{n}(-1)^{n-k}\mathrm{e}^{k\rho}\left[\frac{(k\rho)^{n-k}}{(n-k)!}+\frac{(k\rho)^{n-k-1}}{(n-k-1)!}\right],\ n \geq 2 \end{cases} \tag{8}$$

As the queue grows, there will be an increased probability of droplet coalescence. Specifically, when there are n droplets waiting in the queue, the coalescence rate can be determined according to the Smoluchowski equation (*26*, *27*)

$$\frac{\mathrm{d}n}{\mathrm{d}t} = -8\pi r_c D n^2 \exp(-\Delta G/RT) \tag{9}$$

where r_c is the critical distance between two droplets when attraction begins (m), D is the particle diffusion coefficient (m^2/s), ΔG is the activation energy barrier that must be overcome for the coalescence of two droplets (kJ/kmol droplets), R is the universal gas constant (kJ/kmol/K), and T is the fluid temperature (K).

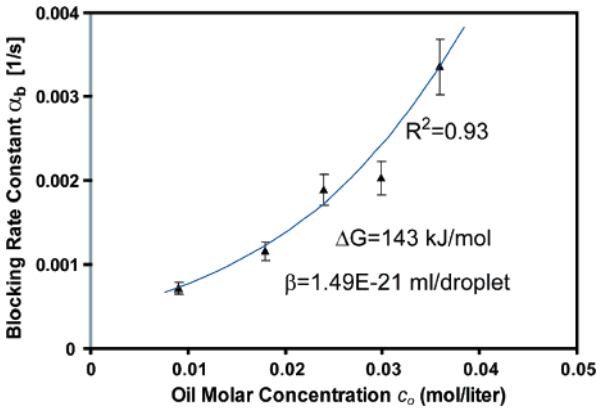

FIGURE 3. Comparison of pore blocking rate constant (α_b) obtained from model predictions (dashed line) and flux observations (dots) at different oil molarities.

Combining the queueing process and emulsion coalescence kinetics, the pore blocking rate constant α_b can be expressed as (see the Supporting Information for details)

$$\begin{aligned} \alpha_b &= -\exp(-\Delta G/RT) \cdot \sum_n 8\pi r_c D n^2 p_n b_n \\ &= -\chi \cdot \exp(-\Delta G/RT) \end{aligned} \tag{10}$$

where b_n is the probability that a pore is blocked when n droplets are waiting in the queue and χ (1/s) is a lump parameter dependent on queueing characteristics and droplet concentration.

To experimentally verify eq 10, a representative semisynthetic MWF called **M0** (see the Supporting Information Table S.2 for composition) was microfiltered through 0.8 μm polyvinylpyrolidone coated polycarbonate membranes. The MWF concentrate was diluted in deionized water at ratios of 1:40, 1:20 1:15, 1:12, and 1:10, resulting in corresponding oil concentrations of 0.008, 0.016, 0.024, 0.030, and 0.036 M that are representative for oil concentrations found in semisynthetic MWFs. In practice, semisynthetic MWFs are always diluted by a factor of 10 or more before use. An undiluted semisynthetic MWF is called a "concentrate" and is not of interest in the context of microfiltration recycling. It was determined by photon correlation spectroscopy that the mean droplet diameter for all the diluted fluids was approximately 20 nm. ΔG and β were calibrated using eq 10 and flux data from two microfiltration experiments (0.08 M and 0.36 M). Based on these calibration experiments, the activation energy ΔG was estimated to be 143 kJ/kmol. This value is consistent with the values of ΔG (100−1000 kJ/kmol) reported by Yamaguchi et al. (*28*) for related lipid microemulsions. As shown in Figure 3, eq 10 predicts α_b at different dilution ratios with reasonable agreement. The results suggest that the pore blocking model eq 10 is appropriate for

estimating α_b in eq 1 within the oil concentration range common for semisynthetic MWFs.

4. Surfactant Package Selection

The models of pore constriction (α_c and R^*) and pore blocking (α_b) capture quantitative relationships between surfactant adsorption, emulsion stability, and flux decline for MWF microemulsions in the microfiltration recycling process. The relationships can be unified into a single model by substituting derived expressions for R^* (eq 3), α_c (eq 4), and α_b (eq 10) into eq 1 as follows:

$$J(t) = \frac{\Delta P e^{-[\chi \cdot \exp(-\Delta G/kT)]t}}{R_m}\left[1 - \frac{2R^*_{\max}c}{(k_d/k_a + c)}(1 - e^{-(k_d+k_a c)t})\right]^2 + \frac{\Delta P}{R_m}\left(1 - \frac{2R^*_{\max}c}{(k_d/k_a + c)}\right)^2\left(1 - \frac{\sqrt{2}}{2}\right)\cdot (1 - e^{-[\chi \cdot \exp(-\Delta G/kT)]t})\left(1 + \frac{2\Delta P \psi c_0 t}{{R_m}^2}\left(1 - \frac{2R^*_{\max}c}{(k_d/k_a + c)}\right)^4 \cdot \left(1 - \frac{\sqrt{2}}{2}\right)^2\right)^{-0.5} \quad (11)$$

As in ref *23*, eq 11 is descriptive of semisynthetic MWF microfiltration that occurs under a coaxial mode where the direction of feed and permeation is the same. We show in the Supporting Information (Figure S.7) that coaxial microfiltration flux before the surface film formation occurs (ψ term in model) is strongly correlated with cross-flow microfiltration flux at steady-state ($R^2 = 0.95$). This is to be expected since near the membrane surface, the fluid flows coaxially during cross-flow filtration. Pore constriction and pore blocking occur for both coaxial and cross-flow modes of microfiltration, while film formation is controlled in cross-flow filtration. Therefore, for relevance to cross-flow microfiltration used in MWF recycling applications, we remove the term for surface film formation from eq 11 to arrive at

$$J(t)|_{t=2000} = \frac{\Delta P e^{-[\chi \cdot \exp(-\Delta G/RT)]\cdot t}}{R_m}\left[1 - \frac{2R^*_{\max}c}{(k_d/k_a + c)}\right]^2 \quad (12)$$

We choose 2000 s in eq 12 as the evaluation point for comparison since in ref *23* it was observed that the pore constriction and pore blocking process are well developed at about 2000 s, while flow resistance due to surface film formation is still negligible.

According to eq 12, the flux performance of a MWF microemulsion is dependent on ΔG, $R^*_{\max}$, and k_a/k_d as well as the droplet size of the MWF microemulsion. These parameters are all a function of the surfactant system selected. An analysis of eq 12 yields the following guidelines for the formulation of microfiltration compatible semisynthetic MWFs:

1. Formulate for small emulsion droplet size so that a large number of droplets must coalesce to block pores.

2. Select surfactants that result in high emulsion stability (i.e., with strong repulsion between droplets and larger ΔG). Notably, reducing the concentration of oil would reduce the droplet density and the possibility of coalescense, but this approach would likely impact manufacturing performance (*29*) and is therefore not considered here.

3. Select surfactants that minimally adsorb to membranes (i.e., smaller k_a/k_d ratio and $R^*_{\max}$).

To provide experimental support for these guidelines, we used them to reformulate the MWF **M0** for improved microfiltration performance. Previous research in ref *11* revealed that the emulsion stability of **M0** can be improved by changing its surfactant package comprised of SPS (anionic) and DiIPA (nonionic) to one of alkyldiphenyl oxide disulfonate (anionic) and linear alcohol ethoxylate (nonionic). It was shown that the replacement surfactant package exhibited improved emulsion stability mainly due to the strong repulsive force between droplets introduced by the twin headed structure of the anionic disulfonate (*11*). Moreover, it was noted that the anionic disulfonate has a relatively high hydrophile−lipophile balance (HLB = 26) value compared with SPS (HLB = 7) and that the nonionic alcohol ethoxylate is more water-dispersible than DiIPA. Based on the guidelines above, we hypothesized that these surfactant characteristics should be favorable for increasing flux relative to the surfactant package in **M0**.

To test the assertion regarding the impact of a revised surfactant package on MWF microfiltration flux, the formulation of **M0** was revised to formulation **M1** as shown in the Supporting Information Table S.3. **M1** has the same oil concentration as **M0**; however, it features the substitution of the anionic and nonionic surfactants at concentrations as close to that of **M0** as possible while still achieving a stable emulsion. The emulsion droplet size is approximately the same for both **M0** and **M1** (20 nm ± 3 nm). A comparison of flux vs time data observed for **M0** and **M1** is provided in Figure 4. It is seen that **M1** has a flux at 2000 s that is 2.7 times higher than **M0**. Since it has been shown that flux differences at 2000 s in coaxial microfiltration are highly predictive of steady-state flux differences in cross-flow microfiltration (see the Supporting Information for details), it can be concluded that **M1** is more microfiltration-compatible than **M0**. Figure 4 also reveals that eq 11 can describe the flux decline behavior of **M0** and **M1** with $R^2 > 0.97$. A fit of eq 11 to these data yields estimates of the surfactant package parameters, with **M1** exhibiting higher ΔG, smaller k_a/k_d ratio, and smaller equivalent pore radius reduction $R^*_{\max}$ than **M0**.

The results suggest the possibility of using a novel method to estimate ΔG for microemulsions. Yamaguchi et al. (*28*) estimated the ΔG of lipid microemulsions by using eq 9 and measuring changes in droplet size as temperature was increased. While this method is straightforward and relatively common, it requires the ability to perform precise emulsion droplet sizing under precise temperature control. The microfiltration method for estimating ΔG developed here presents an alternative that encourages droplet coalescence by streamline contraction. The method is much less sensitive to the estimate of emulsion droplet size since the measurement of small changes of droplet size is not needed. This is important since precise measurements of emulsion droplet size are difficult to achieve (*32*).

5. Optimal Surfactant Concentrations For Microfiltration

While eq 12 yields qualitative guidelines for selecting surfactants, it does not provide quantitative guidance regarding the concentrations at which surfactants should be used. Previous research in ref *11* has shown that for a given surfactant package, MWF microemulsion stability can only be achieved within defined ranges of oil:surfactant molar ratio (ω) and anionic:nonionic molar ratio (θ). For example, Figure 5a shows the stable region for the disulfonate/alcohol ethoxylate surfactant package at all possible oil:surfactant ratios (y-axis) and anionic:nonionic molar ratios (x-axis) that stabilize a naphthenic petroleum oil at 0.018 M concentration. In this research the stable region is operationally defined as combinations of oil:surfactant ratio and anionic:nonionic ratio that lead to fluids that have no observable change in droplet diameter over the period of 1 week using photon correlation spectroscopy. Formulation **M1** corresponds to $\omega = 0.80$ and $\theta = 0.22$, and Figure 5a indicates a flux at 2000 s 2.7 times higher than **M0**, corresponding with the results provided in Figure 4.

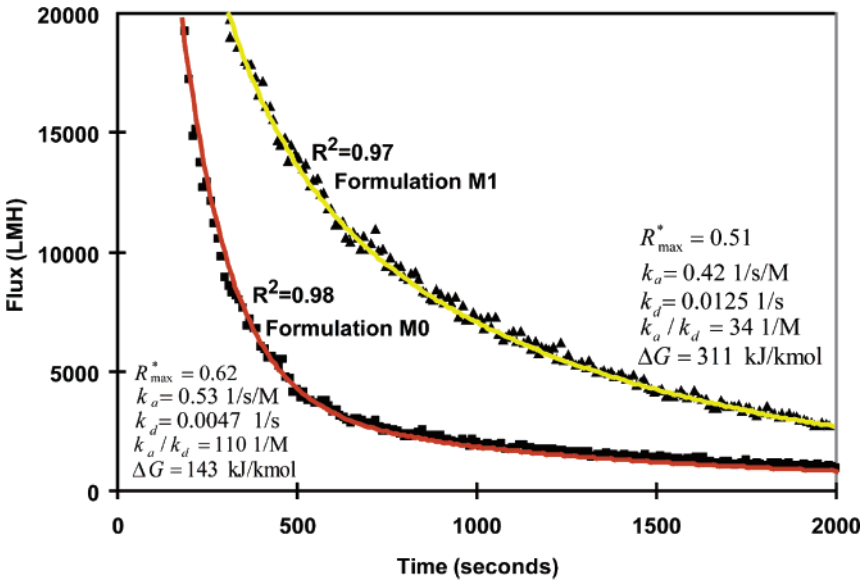

FIGURE 4. Comparison of microfiltration flux data and estimated formulation parameters for MWFs M0 (Supporting Information Table S.2) and M1 (Supporting Information Table S.3).

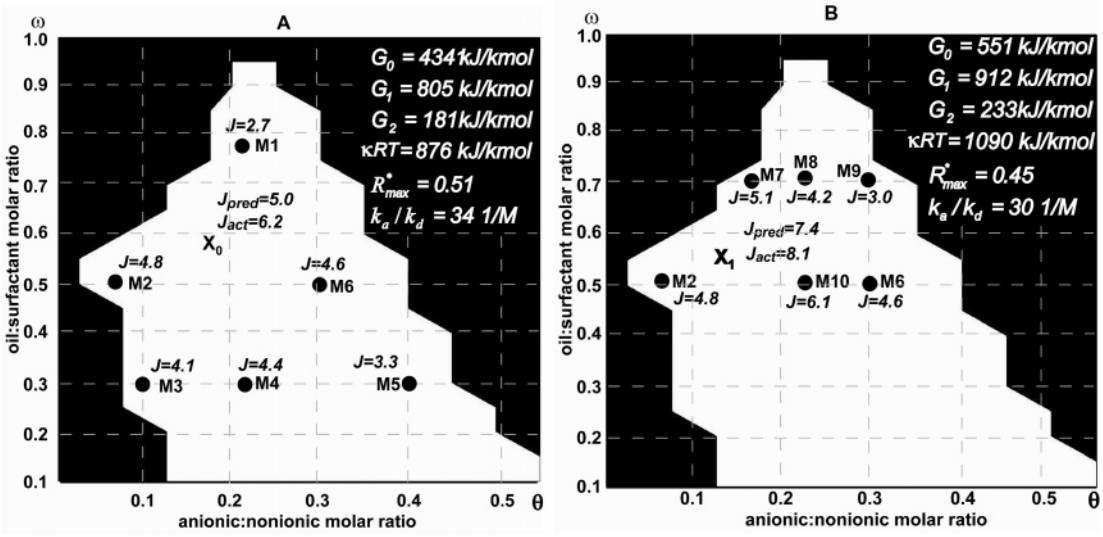

FIGURE 5. Finding optimal disulfonate/ethoxylate concentrations to maximize MWF flux using eq 16. The white region is the stable region and the dark region is the unstable region. (A) Initial experimental design and (B) additional experiments (M7−M10) more closely surrounding the expected optimum in order to improve the predictions of the optimal surfactant concentrations.

To derive an expression that yields the optimal anionic and nonionic surfactant concentrations for maximizing the microfiltration flux of this surfactant mixture, the total surfactant concentration c in eq 11 is first expressed as

$$c = \frac{c_0}{\omega} \tag{13}$$

Then, following the results of (*30*) for a binary surfactant mixture, the coalescence activation energy ΔG is expressed as

$$\Delta G = G_0 - \left[\frac{\theta}{1+\theta}G_1 + \frac{1}{1+\theta}G_2 + \kappa RT\left(\frac{\theta}{1+\theta}\ln\frac{\theta}{1+\theta} + \frac{1}{1+\theta}\ln\frac{1}{1+\theta}\right)\right] \tag{14}$$

where G_0 is the threshold free energy when droplet coalescence occurs, G_1 and G_2 are the nominal free energy values when the surfactants are applied individually, and κ is a proportionality constant that determines the synergistic effect between the surfactants. When a surfactant mixture is used, the free energy decreases in accordance with lower surface tension at the oil−water interface. This leads to a higher ΔG. To evaluate the impact of surfactant concentrations on pore constriction and pore blocking, eqs 13 and 14 are substituted into eq 12. The resulting pore constriction and blocking model becomes

$$J(t) = \frac{\Delta P e^{-\{\chi\cdot\exp[\{(\theta/1+\theta)G_1+(1/1+\theta)G_2+\kappa RT\{(\theta/1+\theta)\ln(\theta/1+\theta)+(1/1+\theta)\ln(1/1+\theta)\}-G_0\}/\omega RT\}t}}{R_m} \times \left[1 - \frac{2\cdot R^*_{\max} c_o}{(k_d/k_a\omega + c_o)}\right]^2 \tag{15}$$

The optimal surfactant concentrations can be determined by taking derivatives on $J(t)$ from eq 14 with respect to ω and θ and then solving the following system of equations:

$$\nabla J = 0 \Rightarrow \begin{cases} \dfrac{\partial J}{\partial \omega} = 0 \\ \dfrac{\partial J}{\partial \theta} = 0 \end{cases} \tag{16}$$

The solution to this set of equations reveals the surfactant concentrations that maximize the microfiltration flux of a given microemulsion at a fixed oil concentration. The solution of equation system 16 results in the following iteration formulas that yield optimal values of anionic:nonionic molar ratio (θ^*) and oil:surfactant molar ratio (ω^*) for maximizing microfiltration flux and

$$\theta^* = \frac{1}{1 + e^{[\omega^* \chi (G_1 - G_2)]/\kappa RT}} \tag{17}$$

$$\omega^* = \frac{1 + \theta^*}{\theta^*(G_1 + G_2)} \times \left\{ RT \ln \frac{4k_a R^*_{max} c_o (1 + \theta^*)}{\chi(\omega^* + k_a/k_d C_o)(G_1 + G_2)(2R^*_{max} c_o - \omega^* - k_a/k_d c_o)} - \frac{}{t} \right. \left. \kappa RT \left(\frac{\theta^*}{1 + \theta^*} \ln \frac{\theta^*}{1 + \theta^*} + \frac{1}{1 + \theta^*} \ln \frac{1}{1 + \theta^*} \right) \right\} \tag{18}$$

6. Experimental Results and Discussion

Optimal Design of Petroleum Based Microemulsions for Recycling. To demonstrate the utility of eqs 17 and 18, they were applied to MWF formulation **M1** with the goal of maximizing the achievable microfiltration flux by modifying the concentrations of the disulfonate and ethoxylate surfactants. The optimization procedure requires that six microfiltration experiments be conducted to calibrate the model, since the model parameters (G_0, G_1, G_2, κ, R^*_{max}, and k_a/k_d) are not generally known in advance for a given MWF formulation/membrane combination. These six points are strategically placed with uniformity throughout the stable region as shown in Figure 5a. Points **M1**−**M6,** with formulations given in the Supporting Information Table S.3, correspond to the $\omega - \theta$ formulation pairs utilized to calibrate the model parameters in eq 15.

Based on the calibration using formulations **M1**−**M6**, eqs 17 and 18 predict that the maximum microfiltration flux occurs at $\omega^* = 0.58$ and $\theta^* = 0.17$, with a flux 5.0 times higher at 2000 s than that observed for **M0**. This optimum point is labeled as **X0** in Figure 5a. The experimentally observed normalized flux at **X0** is 6.2, signifying a deviation from the prediction of approximately 20%. This deviation can be explained by the large range of ω and θ values used in the calibration experiments and the fact that the parameter values need not be constant throughout the $\omega - \theta$ space. Therefore, it can be expected that a second parameter calibration using points close to **X0** would yield a better estimate of the optimal ω and θ combination. Since **M2** and **M6** were already close to **X0**, only four more experiments were needed to calculate a revised optimum point **X1**. These experiments (**M7**−**M10** with formulations given in the Supporting Information Table S.3) are shown in Figure 5b. For the revised optimum formulation **X1**, the expected value of normalized flux was 7.4, and the actual observed value was 8.1. At this optimal point, the deviation between expected flux and observed flux is less than 10%, despite the highly nonlinear relationship between surfactant concentrations and microfiltration flux as indicated by eq 12. The close agreement demonstrates the usefulness of the design optimization approach to significantly increase microfiltration flux over 8-fold relative to the original MWF formulation **M0**.

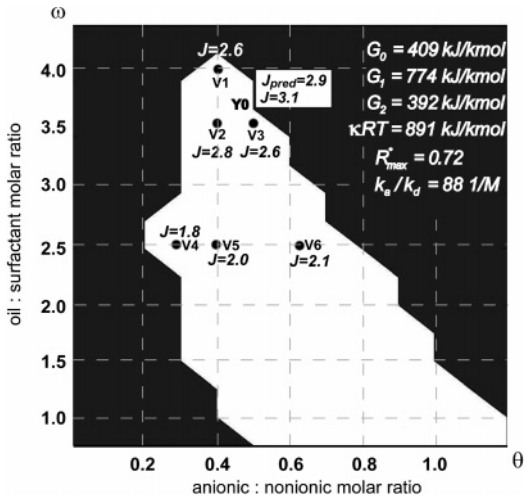

FIGURE 6. Optimization of surfactant concentrations for vegetable oil based semisynthetic MWF formulations using a disulfonate/glyceryl ester surfactant mixture.

Vegetable Oil Based Metalworking Fluids. As a second demonstration of the approach using a different semisynthetic MWF chemistry, we initiated the design of microfiltration-compatible vegetable based semisynthetic MWFs based on the formulation **M1**. The petroleum oil used in **M1** was replaced by one of three vegetable-based lubricants: canola oil, soybean oil, and trimethylolpropane ester. The surfactant combination of disulfonate and alcohol ethoxylate was unsuccessful in emulsifying any of these oils, so the nonionic linear alcohol ethoxylate was substituted with a nonionic ethoxylated glyceryl ester. This nonionic surfactant was selected since it has been previously shown that nonionic surfactants based on glyceryl esters have excellent solubility in vegetable oils while at the same time being dispersive in water (*31*). Therefore, glyceryl esters are good candidates to emulsify vegetable oils together with a disulfonate anionic surfactant. It was found that the combination of anionic disulfonate surfactant and nonionic glyceryl esters was successful in emulsifying all three vegetable oils.

For the disufonate/glyceryl ester surfactant combination, Figure 6 shows the stable ω - θ formulation region for canola oil. Interestingly, this ω - θ stable region was observed to be identical for all three vegetable oils. In addition, all flux observations within the ω - θ stable region were statistically identical for all three vegetable oils. Therefore, the flux and optimization results for canola oil apply equally to all three vegetable oils for the disulfonate/glyceryl ester surfactant combination. For these MWFs, the optimal oil:surfactant ratio (ω^*) is 3.7, and the optimal anionic:nonionic ratio (θ^*) is 0.44 (this formulation is called **Y0**). For **Y0**, the flux model agrees with experimental results to within 7%, with flux 3.1 times higher than M0.

Regarding the economic viability of such flux rates, we note that the long-term average microfiltration fluxes of the metalworking fluids tested in this research are at or above 1000 LMH (liter per square meter membrane area per hour). Generally speaking, we expect that the application of microfiltration to MWF recycling is economically viable if a flux over 100 LMH can be achieved. Even with the introduction of contaminants, it is expected that the flux will remain higher than 100 LMH since external contaminants such as oil, chips, and bacteria can be reasonably controlled using cross-flow microfiltration. The economic analysis of general microfiltration implementation strategies for MWF recycling provided in ref *31* indicates that increase of microfiltration flux can lead to a nearly proportional reduction on overall system cost.

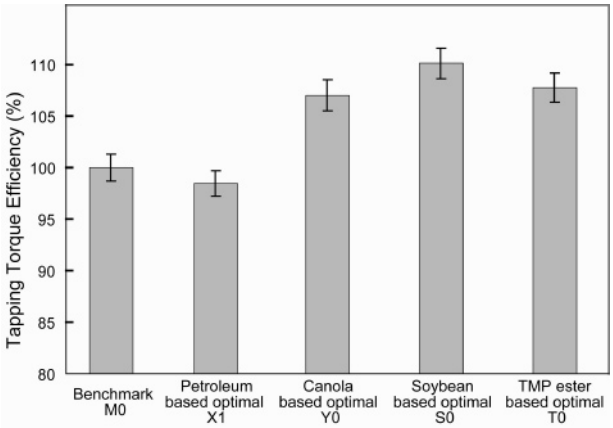

FIGURE 7. Comparison of manufacturing performance for petroleum and vegetable based formulations using the tapping torque test.

Robustness of Microfiltration-Compatible MWFs to Hardwater Ion Accumulation. Hardwater ions accumulate to high concentrations in MWFs since tap water is generally added to replenish water lost to evaporation. Observed hardwater ion concentrations can exceed 500 ppm as $CaCO_3$ (*33*) which can lead to increased microbial concentrations, emulsion splitting, and failure of the MWF so that it must be disposed (*6*, *17*, *34*).

Microfiltration flux was measured for formulations **M0**, **X1**, and **Y0** at Ca^{2+} concentrations up to 500 ppm as $CaCO_3$. It is observed that the microfiltration performance of formulation **M0** deteriorates significantly with even slight increases in hardwater ion concentration. In contrast, formulations **X1** and **Y0** have less than 10% flux decline at Ca^{2+} concentrations below 500 ppm (see the Supporting Information Figure S.6 for details). These observations suggest that steps taken to improve emulsion stability also improve resistance to coalescence and therefore lead to higher MWF flux. We expect that this is because in formulations **X1** and **Y0,** disulfonate surfactant is used to replace sodium petroleum sulfonate. Due to the higher electrostatic charge of disulfonate molecules at the pH of MWF (about 9), microemulsion droplets have inherently increased resistance to coalescence in the presence of hardwater. Also, hardwater ions may associate with disulfonate surfactant to form soluble anionic surfactant-cation complexes at high concentrations (*11*). These mechanisms effectively reduce the pore blocking mechanism, thereby increasing flux, while also reducing the propensity for these MWFs to deteriorate in the field due to accumulation of hardwater ions as observed in ref *11*.

Manufacturing Performance. We conclude by recognizing that the reformulation of MWFs for increased microfiltration flux will not occur if manufacturing performance is compromised. In Figure 7, the MWFs developed during this research are compared using the tapping torque efficiency metric (*35*), where higher efficiency is indicative of improved manufacturing performance. It is observed that for petroleum oil MWFs the optimized microfiltration-compatible fluid (**X1**) has essentially the same manufacturing performance as the benchmark fluid (**M0**). This is expected since manufacturing performance is almost completely determined by oil type and concentration, which we kept unchanged during the rereformulation process. The higher manufacturing performance achieved for vegetable oil based fluids (**Y0**, **S0**, **T0**) relative to the petroleum oil MWFs (**M0**, **X1**) is due to the change of oil type. The higher performance of vegetable oils in MWF applications is well-known and consistent with previous observations reported in literature (*36*, *37*).

Taken together, the results indicate that selecting semisynthetic MWF surfactants for resistance to membrane adsorption and droplet coalescence, while also optimizing surfactant concentrations, not only increases microfiltration flux and reduces the cost of recycling but also produces MWFs that are more robust to deterioration caused by hardwater ion accumulation. This can be achieved without compromising manufacturing performance and thus provides a further means to increase the longevity of MWFs. The results presented in this work are therefore relevant to efforts aimed at reducing MWF life-cycle environmental impact as well as costs associated with MWF acquisition and disposal.

Acknowledgments

This research was funded by the National Science Foundation under Contract No. DMII-0093514. The contents of this publication have not been subject to Agency review and therefore do not necessarily reflect the views of NSF. The metalworking fluid components used were generously provided by Cargill, Inc. (Chicago, IL), Degussa, Inc. (Hopwell, VA), Dow Chemical Company (Midland, MI), Milacron, Inc. (Cincinnati, OH), Tomah Products (Reserve, LA), and Uniqema, Inc. (New Castle, DE). The authors also wish to acknowledge Professors Kim Hayes and Julie Zimmerman for their roles in previous research contributing to this investigation and Marcy Urbance and Carlos Aguilar for their contributions to experimental testing.

Supporting Information Available

Details on the MWF microfiltration mechanistic model and experimental validation leading to eq 1, derivation of the pore constriction and pore blocking models developed in sections 2 and 3, and experimental materials and methods. This material is available free of charge via the Internet at http://pubs.acs.org.

Literature Cited

(1) Sheng, P. Life-cycle Planning of Cutting Fluids—A Review. *J. Manuf. Sci. Eng.* **1997**, *119* (4B), 791−800.
(2) Sutherland, J. et al. CFEST: An Internet-based Cutting Fluid Evaluation Software Testbed. *Trans. NAMRI/SME* **1997**, *25* (5), 243−248.
(3) *Metalworking Fluids*; Byers, J. P., Ed.; Marcel Dekker, Inc.: New York, 1994.
(4) Independent Lubricant Manufacturers Association. ILMA Report on the Volume of Lubricants Manufactured in the United States and Canada by Independent Lubricant Manufacturers. In *Lubricants World*; 2000; p 10.
(5) Klocke, F. et al. Dry cutting. *Ann. CIPP* **1997**, *46* (1), 1−8.
(6) National Institute of Occupational Safety and Health. *Criteria for a Recommended Standard: Occupational Exposure to Metalworking Fluids*; Cincinnati, OH, 1998.
(7) Rossmoore, H. W. Microbiology of Metalworking Fluids: Deterioration, Disease and Disposal. *Lubr. Eng.* **1995**, *51* (2), 113−130.
(8) Skerlos, S. J. et al. Environmentally Conscious Disposal Considerations in Cutting Fluid Selection. In *Proceedings of the ASME: Manufacturing Science and Engineering Division*; Lee, J., Ed.; Anaheim, CA, 1998; Vol. 8, pp 397−403.
(9) U.S. Environmental Protection Agency. *Effluent Limitations Guidelines and New Source Performance Standards for the Metal Products and Machinery Point Source Category*; EPA 40 CFR Part 438, 2003.
(10) Graham, D. Going Dry. *Manuf. Eng.* **2000**, *124* (1), 4−5.
(11) Zimmerman, J. B. et al. Design of Hard Water Stable Emulsifier Systems for Petroleum and Bio-based Semi-synthetic Metalworking Fluids. *Environ. Sci. Technol.* **2003**, *37* (23), 5278−5288.
(12) Cheryan, M. *Ultrafiltration and Microfiltration Handbook*; Technomic Publishing Company, Inc.: Lancaster, PA, 1998.
(13) Janknecht, P. et al. Removal of Industrial Cutting Oil from Oil Emulsions by Polymeric Ultra- and Microfiltration Membranes. *Environ. Sci. Technol.* **2004**, *38* (18), 4878−4883.
(14) Marchese, J. et al. Pilot-scale ultrafiltration of an emulsified oil wastewater. *Environ. Sci. Technol.* **2000**, *34* (14), 2990−2996.
(15) UTCIS-WRAP. The University of Tennessee Center for Industrial Services Waste Reduction Assistance Program, New Ultrafiltration Unit Reduces Waste, Saves Money for TRW. *WRAPSHEET* **1997**, *7* (2), 1−5.

(16) Mahdi, S. M. Sköld, R. O. Experimental Study of Membrane Filtration for the Recycling of Synthetic Waterbased Metalworking Fluids. *Tribol. Int.* **1991**, *24* (6), 389−395.
(17) Rajagopalan, N. et al. Purification of Semi-synthetic Metalworking Fluids by Microfiltration. *Tribol. Lubr. Technol.* **2004**, *60* (8), 38−44.
(18) Sato, H. et al. Cross-flow Filtration of Machining Fluids by Microfiltration Membranes (Influence of Chip Size on Permeation Flux). *JSME Int. J., Ser. C* **1996**, *39* (3), 636−644.
(19) Koltuniewicz, A. B. Field, R.W. Process factors during removal of oil-in-water emulsions with cross-flow microfiltration. *Desalination* **1996**, *105* (1−2), 79−89.
(20) Cakl, J. et al. Effects of Backflushing Conditions on Permeate Flux in Membrane Crossflow Microfiltration of Oil Emulsion. *Desalination* **2000**, *127* (2), 189−198.
(21) Tarleton, E. S. How electric and ultrasonic fields assist membrane filtration. *Filtr. Sep.* **1988**, *25* (6), 402−406.
(22) Skerlos, S. J. et al. Ingredient-wise Study of Flux Characteristics in the Ceramic Membrane Filtration of Uncontaminated Synthetic Metalworking Fluids. *J. Manuf. Sci. Eng.* **2000**, *122* (4), 739−752.
(23) Zhao, F. et al. Mechanistic Model of Coaxial Microfiltration for a Semi-Synthetic Metalworking Fluid Microemulsion. *J. Manuf. Sci. Eng.* **2004**, *126* (3), 435−444.
(24) Skerlos, S. J. et al. Model of Biomass Concentration in Membrane Filtration Recycling Systems Subject to Single Substrate Limited Growth Kinetics, Proceedings of the ASME: Manufacturing Science and Engineering Division. Orlando, FL, 2000; Vol. 10 (11), pp 813−820.
(25) Gross, D.; Harris, C. M. *Fundamentals of Queueing Theory;* John Wiley & Sons, Inc.: New York, 1974.
(26) Myers, D. *Surfaces, Interfaces, and Colloids*; VCH Publishers: New York, 1990.
(27) Adamson, A. W.; Gast, A. P. *Physical Chemistry of Surfaces*, 6th ed.; John Wiley & Sons, Inc.: New York, 1997.
(28) Yamaguchi, T. et al. Physicochemical Characterization of Parenteral Lipid Emulsion: Determination of Hamaker Constants and Activation Energy of Coalescence. *Pharm. Res.* **1995**, *12* (3), 342−347.
(29) Newton, J. Look at Lubricating Oils. *Ind. Lubr. Tribol.* **1989**, *41* (1), 13−15.
(30) Razavizadeh, B. M. et al. Thermodynamic Studies of Mixed Ionic/nonionic Surfactant Systems. *J. Colloid Interface Sci.* **2004**, *276* (1), 197−207.
(31) Skerlos, S. J., et al. Economic Considerations in the Implementation of Microfiltration for Metalworking Fluid Biological Control. *J. Manuf. Syst.* **2003**, *22* (3), 202−219.
(32) Becher, P. *Emulsions: Theory and Practice*, 3rd ed.; Oxford University Press, Inc.: New York, 2001.
(33) IAMSI. *Institute of Advanced Manufacturing Sciences Incorporated, Pollution Prevention Guide to Using Metal Removal Fluids in Machining Operations*; Cincinnati, OH, 1995.
(34) Zimmerman, J. et al. Influence of Ion Type and Concentration on the Emulsion Stability and Machining Performance of Two Semi-Synthetic Metalworking Fluids. *Environ. Sci. Technol.* **2003**, *38* (22), 2482−2490.
(35) Zimmerman, J. B. et al. Experimental and Statistical Design Considerations for Economical Evaluation of Metalworking Fluids Using the Tapping Torque Test. *Lubr. Eng.* **2003**, *59* (3), 17−24.
(36) Clarens, A. F. et al. Experimental Comparison of Vegetable and Petroleum Base Oils in Metalworking Fluids using the Tapping Torque Test. *Proceedings of the Japan/USA Symposium on Flexible Manufacturing*, Denver, CO, July 2004; pp 19−21.
(37) Honary, L.; Boeckenstedt, R. Making a Case for Soy-Based Lubricants. *Lubr. Eng.* **1998**, *54* (7), 18−20.

Received for review April 4, 2006. Revised manuscript received October 24, 2006. Accepted October 31, 2006.

ES0608038